UNIABUJA Journal of Engineering and Technology

https://ujet.uniabuja.edu.ng/

ISSN: 2714-3236 (Online); 2714-3228 (Print)

Volume 3, Issue 1, 2026; 240-249

Design Modification of Domestic Solar Water Storage Tank with Central and Circumferential PCM for Performance Improvement

Kafayat ADEYEMI[1], Musa T. ZARMAI[2], Lawal M. NASIR[3*], Roberts I. BOLAJI[4]

[1,2,3*]*Department of Mechanical Engineering, University of Abuja, Abuja, Nigeria*
[4]*Communal Integrated Services, FCT Abuja, Nigeria*

[1]*kafayat.adeyemi@uniabuja.edu.ng*, [2]*musa.zarmai@uniabuja.edu.ng*, [3*]*nasir.lawal@uniabuja.edu.ng*, [4]*communalitegratedservices@gmail.com*

Abstract

This study experimentally investigates enhancing a domestic solar water storage tank's thermal performance by integrating phase change materials (PCMs) in central (C-PCM), circumferential (A-PCM), and dual (C+A-PCM) configurations. A control tank without PCM was used for comparison. Results demonstrated that the circumferential PCM arrangement (A-PCM) performed optimally, improving heat retention by 73% over the control due to its superior surface-area-to-volume ratio, which extended hot water availability. The dual-PCM system offered only a marginal gain of 8% over the A-PCM configuration, while the central PCM (C-PCM) lagged significantly due to limited thermal interaction. These findings align with previous research on annular PCM geometries. Economically, the high initial capital cost for PCM integration remains a challenge. However, the system's projected payback period is 2.3 years, with a lifetime return on investment exceeding upfront by 220%, indicating strong long-term viability. The study concludes that a circumferential PCM configuration is the most effective and economically motivating design for improving thermal energy storage in residential solar thermal systems.

Keywords: *Central and circumferential PCM, annular water-body, concentric cylinders, charging and discharging cycles, design modification.*

1.0 Introduction

Solar thermal systems (STS) address global energy demands by converting sunlight into heat, particularly for water heating [1]. A key limitation is the temporal mismatch between solar availability and demand, necessitating efficient thermal energy storage (TES) [2]. Conventional sensible heat storage (SHS) systems exhibit low energy density and significant heat losses [3]. Phase change materials (PCMs) offer transformative potential, storing 5 - 14 times more energy per unit volume and stabilizing temperatures [4].

Recent studies show PCM integration in solar water heaters (SWHs) improves thermal retention. Sharma et al. [5] reported 18 - 22% efficiency gains via PCM embedding. However, conventional configurations (e.g., horizontal layers) suffer from poor heat transfer and uneven distribution [6 - 7]. Dual PCM positioning (central + circumferential) addresses these issues: central modules enhance core heat exchange, while circumferential layouts leverage surface area for faster charging/discharging [8]. Al-Hinti et al. [9] noted 30% improved thermal diffusion with radial placement, and Korti et al., [10] reported 12 - 15% reduced charging times in hybrid systems.

Despite progress, synergistic effects of combined PCM layouts under realistic solar variability remain underexplored. This study proposes a modified tank design with dual PCM configurations to enhance energy density, reduce losses, and extend discharge in tropical climates.

In tropical regions like Abuja, Nigeria (solar irradiance: 5.5–6.5 kWh/m²/day [11]), high ambient temperatures (28 - 35°C [12]) reduces thermal gradients between the fluid and the environment, hence lowering heat retention capacity [13]. Water-based SHS limits energy density, requiring oversized tanks [14]. Existing PCM systems are poorly optimized: horizontal layers exhibit incomplete phase transitions (40–60% utilization [15]), and humidity (>70% [18]) accelerates corrosion [16]. Paraffin-based PCMs often mismatch tropical temperatures, causing premature melting [17], while circumferential designs suffer from condensate-induced conductivity losses [18]. These issues lead to suboptimal efficiency (15–25% below projections [19]).

This study develops and evaluates a dual-PCM storage tank (central + circumferential) to improve thermal efficiency, energy density, and operational duration in tropical climates, addressing critical gaps in heat retention and stratification [9,10].

2. Methodology

This covers the materials used, design specifications, PCM configuration and Analysis of heat transfer.

Received: 17-12-2025 / Accepted: 24-12-2026 / Published: 14-03-2026

https://doi.org/10.70118/ujet.2026.0301.22

2.1 Materials and Software Tools

A 160 lt stainless steel (AISI 304) storage tank was selected for corrosion resistance in a tropical region such as Abuja, Nigeria (9.0563° N, 7.4985° E) [20]. Insulation was 54 mm polyurethane foam (k=0.023 W/m·K) [21]. Two PCMs were integrated: a central aluminium cylinder with Paraffin wax (RT50, 56 °C) [22, 23], and a circumferential annular ring of Eutectic salt ($CaCl_2 \cdot 6H_2O$, 190 kJ/kg) for humidity stability [24]. Solid-works version 2024, MATLAB 2016-R2 and Excel were the software used in modelling and system simulation.

2.2 Design Modification

The tank was designed to API-650 standards for 150 - 200 Lt Capacity at 70 °C and 1.014 bar. Materials were galvanized steel (cover) and mild steel (bracket), with a 3.2 mm corrosion allowance (ASME B31-3). The strategy involves use of two positioned PCM – one at the centre and the other at the circumference to be charged during the day time and discharge during the night.

2.2.1 PCM Geometric Sizing

The PCMs are concentrically arranged as shown in Figure 1, with the central PCM – 1, having a diameter of 100 mm and enclosed with an aluminium cylinder of metal plate thickness t_a= 1.5 mm. The circumference PCM – 2, is an annular compartment enclosed with inner cylinder plate - 1, and an outer cylinder plate – 2, of the same thickness and same height H = 765 mm. See the fabrication processes in Figures 3 and 4.

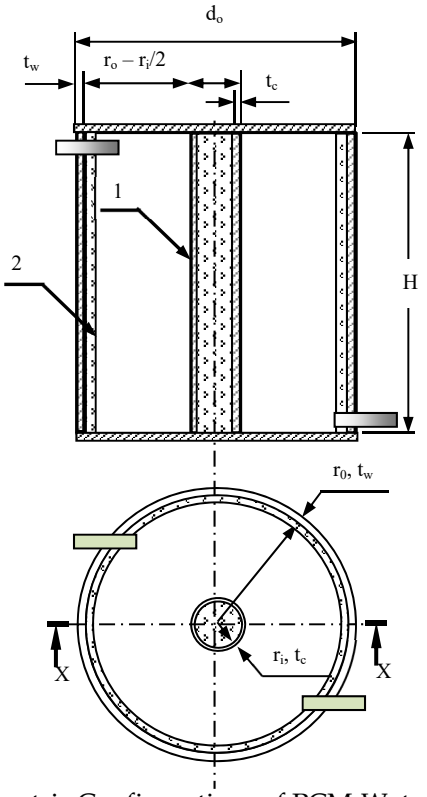

Figure 1: Geometric Configurations of PCM-Water-PCM Concentric Cylinders

2.2.2 Heat Transfer Governing Equations

The Energy balance Equation for the heat transfer is given in Equation 1 as:

$$Q_w = m_w C_w \Delta T \quad (1)$$

where; Q_w = Quantity of Heat transferred during charging or discharging, m_w = mass of water, C_w = Specific heat capacity of water and ΔT = Change in temperature of water.

The temperature gradient is given in Equation 2, [26]:

$$\frac{dT_w}{dt} = \frac{Q_s - Q_l - Q_{pcm}}{m_w C_{p,w}} \quad (2)$$

$$\text{where: } Q_{pcm} = h_{pcm} A_{pcm} (T_w - T_{pcm}) \quad (3)$$

WhereQ_s = heat from solar panel,h_{pcm} = forced convective heat transfer of water-PCM [27].

The PCM Phase-Change thermal model is described by streamlined Navier-Stroke equation given in Equation 4 [26].

Received: 17-12-2025 / Accepted: 24-12-2026 / Published: 14-03-2026

https://doi.org/10.70118/ujet.2026.0301.22

$$\frac{\partial H}{\partial t} = k_{pcm}\nabla^2 T + \rho_{pcm} L\frac{\partial f}{\partial t} \quad (4)$$

where: k_{pcm} = thermal conductivity of PCM, f = liquid fraction, L = latent heat as provided.

2.2.3 Geometric Sizing of the Water Annulus

The tank was considered to have radii ri and ro and thickness tc and tw for the inner cylinder and outer cylinder respectively. The volume of the central PCM is given in Equation 5.

$$V_c = \pi r_i^2 H \quad (5)$$

where V_c = the volume of the central PCM, r_i = radius of the inner PCM cylinder and H = the height of the cylinder.

The volume of the annulus of water is given in Equation 6.

$$V_w = \pi[(r_o - t_w)^2 - (r_i + t_c)^2]H \quad (6)$$

where: V_w = volume of water in the annulus,r_o = is the outer radius of the circumferential PCM, t_w = is the thickness of the outer container metal plate and t_c = is the thickness of the inner container metal plate.

The shell thickness given in Equation 7 was based on API 650 design Clause 3.4.1 [29].

$$t_s = 2.6d_o(H - 1) * G * E * S + CA \quad (7)$$

where, D = internal diameter of the tank, H = maximum height of water level, G = specific gravity of water and E = joint efficiency, S = tensile stress and CA = corrosion allowance.

The diameter of the encapsulating PCM is given in Equation 8.

$$d = \sqrt{4\frac{m_w C_w \Delta T - Q_l}{\pi \rho_p L_p^2}} \quad (8)$$

where m_w = mass of water, C_w = specific heat capacity of water, ΔT = change in temperature, Q_l = Latent heat of PCM, ρ_p = density of PCM and L_p= Latent Heat of PCM.

2.2.4 Modification Implementation Processes

The first part of the development process was to produce the working drawing for the modified water heater tank. This was followed with material selection for the components, then the construction and assembly and finally, performance evaluation.

i. The model drawings contain four parts as shown in Figure 2:

a. Isometric view of the Tank: it represents the outer components of the tank with both central and circumferential cylinders and inlet and outlet piping. It has a total height of 612 mm to ensure the PCM is submerged completely.

b. The central PCM Container: it is made of aluminum, a length of 612 mm, diameter of 200 mm and a thickness of 1.5 mm.

c. The circumferential cylinder of the PCM: there are two cylinders separated by a 5 mm gap: the outer one has an external diameter of 446 mm and the inner one has an inner diameter of 430 mm. The tank has a nominal height of 765 mm and plate thickness of 1.5 mm

d. Assembly view of the tank: contains sectional views of the elevation and plan with the hidden details such as insulation thickness (54 mm) and the insertion cover plate is 150 mm secured with six M8 bolts.

Received: 17-12-2025 / Accepted: 24-12-2026 / Published: 14-03-2026

https://doi.org/10.70118/ujet.2026.0301.22

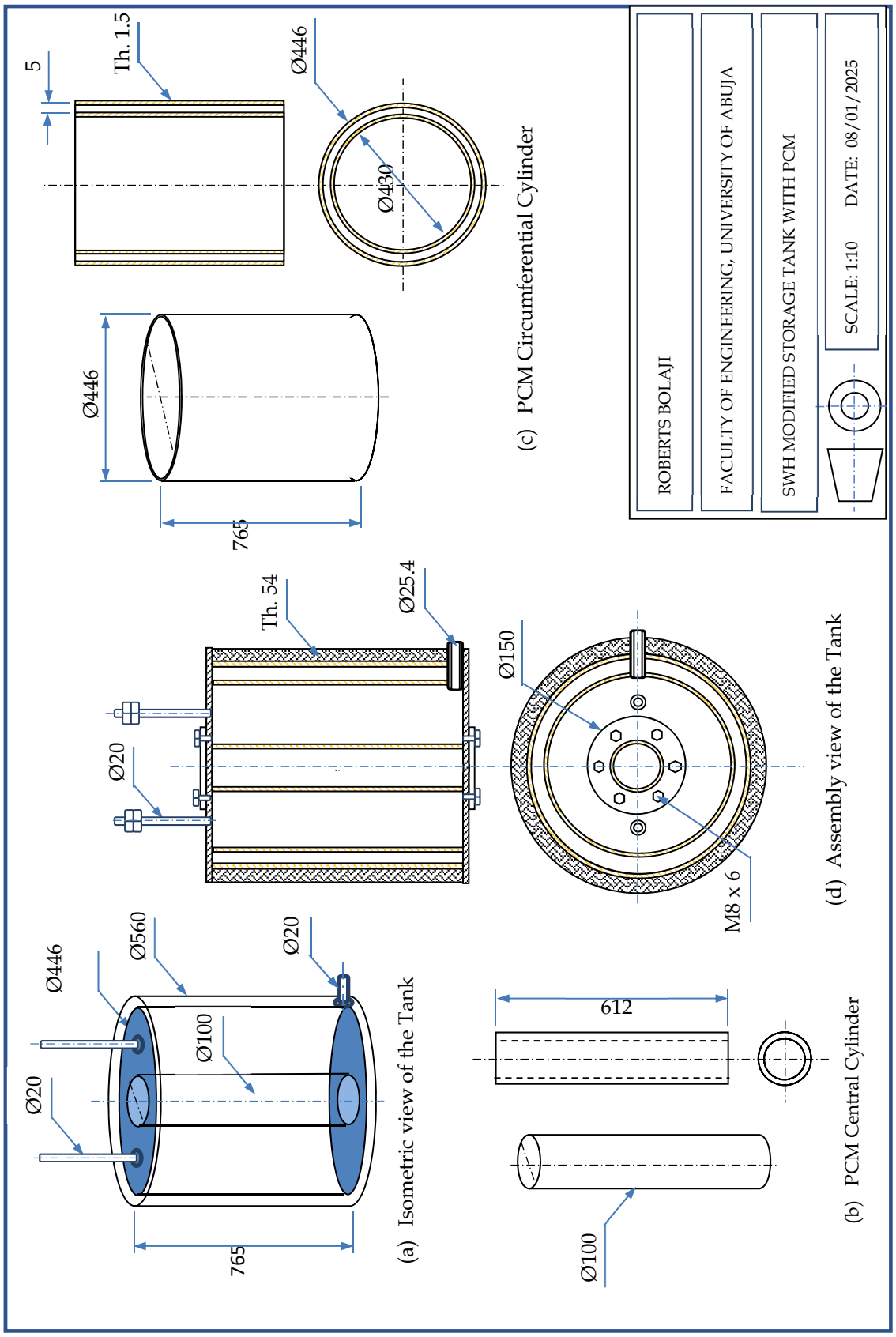

Figure 2: Isometric and Orthographic Drawing of the Modified Tank

Received: 17-12-2025 / Accepted: 24-12-2026 / Published: 14-03-2026
https://doi.org/10.70118/ujet.2026.0301.22

3.0 Material Selection:

Aluminium pipe was used for the central PCM container, due to its high conductivity and resistance to corrosion. The circumferential cylindrical shells, is made from A304 (tensile strength = 485 MN/m2).

3.1 Fabrication of PCM Containers

The fabrication processes of the central and circumferential PCMs are shown in Figures 3 and 4 respectively.

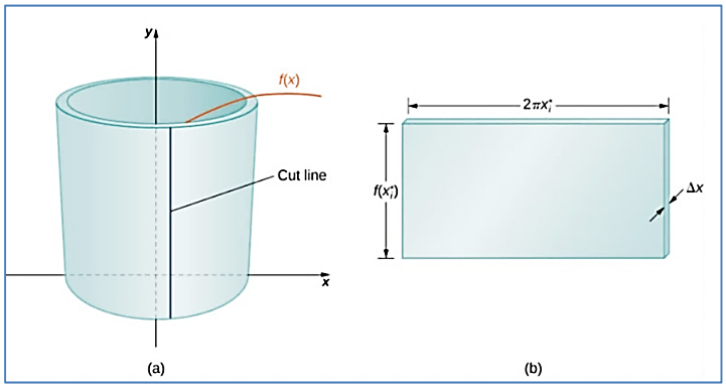

Figure 3: Development of the PCM capsulated Cylinder [30]

The cut-out or development with the circular end covers are shown in Figure 5.

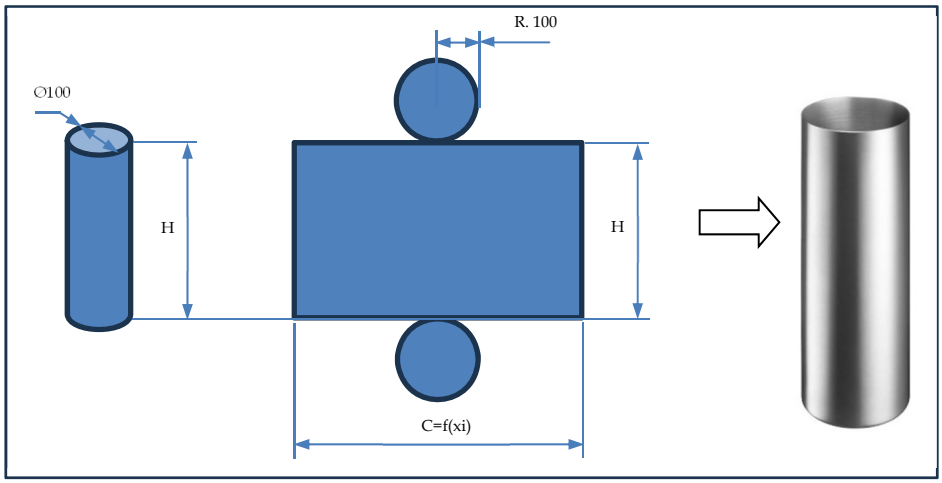

Figure 4: Cutting and folding of the PCM capsule metal sheet

3.2 Insertion of PCM Containers into a Tank

The tank was marked and cut at the center for the capsule PCM and at the bottom plate for the circumference PCM as shown in Figures 5 and 6 respectively.

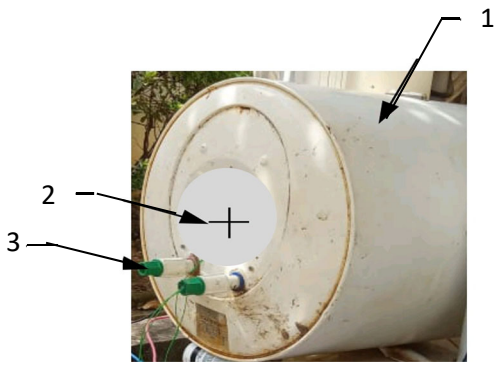

Part #System Description

1. An Existing storage tank shell
2. Plumbing lines disconnected
3. Central point to cut hole to accommodate CPM capsule

Figure 5: Existing hot water tank before modification

Received: 17-12-2025 / Accepted: 24-12-2026 / Published: 14-03-2026
https://doi.org/10.70118/ujet.2026.0301.22

Insertion and sealing of the PCMs are shown in Figure 5

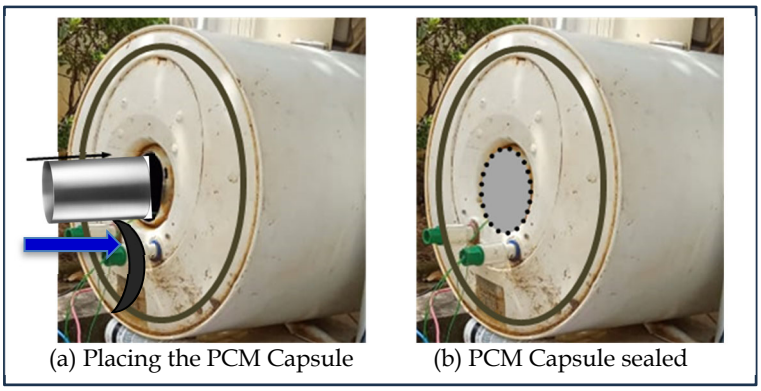

(a) Placing the PCM Capsule (b) PCM Capsule sealed

Figure 6: PCM integration with the Existing Hot Water Tank

3.3 Key components

The key parts of the tank are the modified tank body, PCM containers, insulation, external shell, sensor-fitted pipes, and reinforced 2.5 mm channel frame for added load, details in Table 1.

Table 1: Basic components of a solar hot water tank with PCM

S/N	Component	Material	Specifications	Designed Size
1	Storage Tank Body	Galvanized Steel	Capacity: 160 lt; Max Pressure: 6 bar; Temp Range: 0–100°C	Height: 0.765 m; Diameter: 0.56 m
2	Central PCM & Container	Paraffin Wax encapsulated in Aluminum container	Volume: 4.8lt; PCM Type: Paraffin Wax (Melting Point: 56.5°C)	Height: 0.612 m; Diameter: 0.1 m
3	Peripheral PCM & Layer	Salt hydrates encapsulated in Aluminum container	Volume: 3.7lt; PCM Type: Eutectic salt - $CaCl_2 \cdot 6H_2O$. (Melting Point: 58°C)	Thickness: 0.005 m (around water annulus)
4	Insulation Layer	Polyurethane Foam	Thickness: 54 mm; Thermal Conductivity: 0.022 W/mK	Covers entire tank
5	External Shell	Galvanized Steel	Thickness: 1.5 mm; Corrosion-resistant coating	Height: 0.768 m; Diameter: 0.56 m
6	Inlet/Outlet Ports	Stainless Steel	Diameter: 25 mm (1"); Threaded Connections	2 ports (top and bottom)
7	Temperature Sensors	Digital Sensors	Range: 0–100°C; Accuracy: ±1 °C; 2 Sensors (central and peripheral PCM monitoring)	NA
8	Pressure Relief Valve	Brass	Set Pressure: 6 bar; Temperature Rating: 100°C	25 mm diameter
9	Mounting Brackets	Mild Steel	Powder-coated for durability; Load Capacity: 500 kg	Length: 1.5 m, thickness: 2.5 mm (total support structure)

3.4 Experimental Setup

The system (Figure 7) includes pump-1 supplying cold water (0.25 lt/s, 25 °C) to solar panel-2 tilted at 15° for solar exposure (8 am - 6 pm). To keep the system steady and conserved, heated water from the solar panel enters the storage tank and leaves the tank at the same rate.

Received: 17-12-2025 / Accepted: 24-12-2026 / Published: 14-03-2026
https://doi.org/10.70118/ujet.2026.0301.22

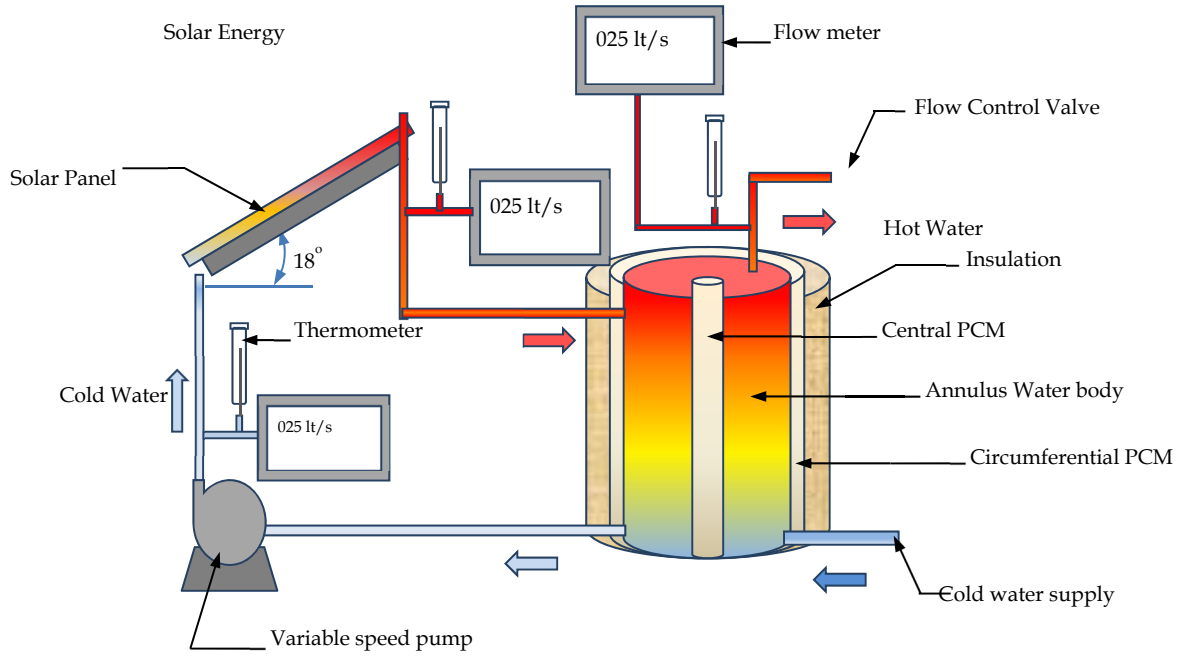

Figure 7: Experimental set up for Performance Evaluation

Thermometers and flow-meters are installed at inlet and outlet of each unit to measure the temperature and flow rate at preset time intervals over the periods of tests.

3.4.1 Instrumentation and Testing Conditions

Three major instruments were used, (i) PT1000 RTD temperature sensor (–20°C to 150°C, ±0.5°C accuracy, ±0.1°C resolution, IEC 60751), (ii) differentialcontroller (3–15°C range, ±1.0°C accuracy, 0.1°C resolution. Overheat protection at 85°C ±2°C) and turbine flow-meter (0.5–10 L/min, ±2% accuracy, 0.1 lt/min resolution).

The testing conditions are: (i) charging: 4 hours (10 AM–2 PM, simulated irradiance) and (ii) discharging: 6 hours (6 PM–12 AM, 30°C ambient, 70% RH).

3.4.2 Procedures

Testing Protocols were based on ISO 9806 [28].Four tests under identical solar input were conducted (at least 5 times per test), namely: (i) baseline without PCM, (ii) central PCM only, (iii) circumferential PCM only and (iv) dual PCM.

In each case, the tests started with initial water temperature T_1 and the water heated to 80°C. It was then isolated and temperatures T_x measured at intervals time t_x. Heat loss rate was determined from $\Delta T_x = T_1 - T_n$. Key factors investigated here are insulation, ambient T_{ax}, tank size, water properties.

3.4.3 Data Collection and Validation

Temperatures were recorded based on the recommendations of ANSI/ASHRAE 94.1-2022 [29]. Efficiency was calculated via ISO 9459-2:2021 [16], while numerical analyses for gradient and heat loss were done using (MATLAB FEM) and validation done with an RMSE ≤ 5% (experimental versus simulated).

4.0 Results and Discussion

The results cover design parameters, environmental impacts, circumferential PCM influence, and statistical reliability.

4.1 Design Parameters and Material Selection

The basic design parameters are the tank nominal diameter and height which are 560 mm and 765 mm respectively. These values are chosen to give a volume of about 160 Lt to support a family size of six as advised in [13]. The metal plates are 1.5 mm in thickness and the insulation thickness is 54 mm made of polyurethane foam. The PCM are paraffin wax at the center and Eutectic salt ($CaCl_2 \cdot 6H_2O$) at the circumference together occupying about 5.3% of the total volume. The dual PCM enhances energy density by 30%, despite its smaller volume.

Comparative Size of the PCM: The temperature profiles of two models are shown in Figure 8, the trend in blue is for the current model while the one in red is for an existing system used for comparison. This is important to ensure that the central and circumferential PCM have the right workable thickness.

Received: 17-12-2025 / Accepted: 24-12-2026 / Published: 14-03-2026

https://doi.org/10.70118/ujet.2026.0301.22

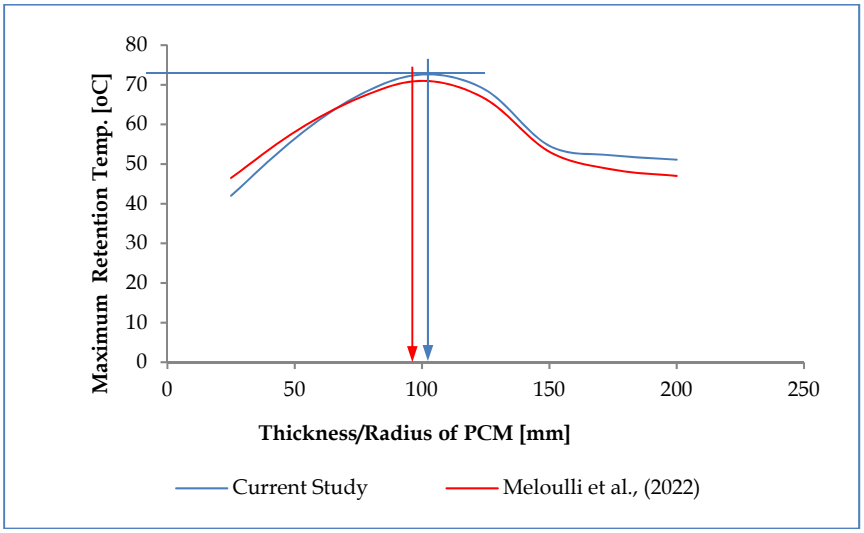

Figure 8: Temperature of the PCM versus PCM Dimension

From the graph, thecentral PCM produces maximum retention temperature 71.8 ^{o}C when the cylinder diameter is Ø100 mm with 80% of tank height for complete immersion for full tank resulting to a total volume of 4.8 lt. The circumferential PCM on the other hand occupies an annular space of 5 mm resulting to 3.7 lt. the combined volume of 8.5 lt represents 5.3% of the tank volume, which far less than the allowable limit of <15% PCM of the tank capacity.

4.2 Influence of Circumferential PCM on Heat Distribution and Retention

The heat distribution for each type scenario of CPM placement: 1 – central placement only (C-PCM), 2 – Circumferential placement (A-PCM) and 3 – Both Central and Circumferential (C+A PCM) are shown in Figure 9. In each case, the part of the water closest to the PCM is the hottest and the temperature reduces gradually away from the PCM boundary. These situations are shown in the color map in Figure 9.

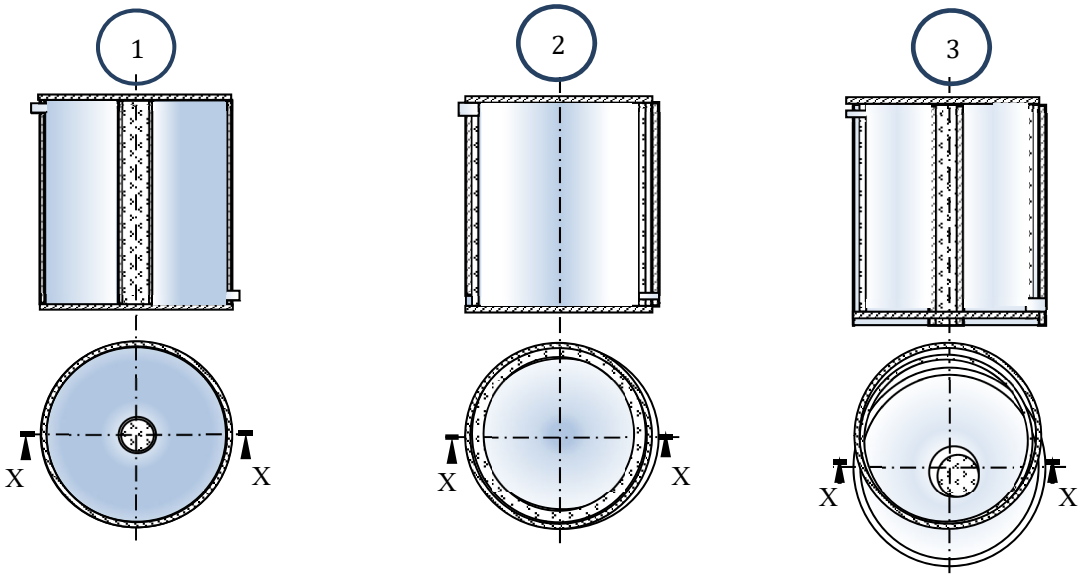

(a) C-PCM at the Center (b) A-PCM at the Circumference (c) C+A PCM at Both Locations

Figure 9: Temperature distribution in the body of water due to heat exchange

From the colour map results, the whitish part indicates heat transfer zones which are highest close to the PCMs. Using Equation 7, the heat retention in each scenario was computed. The central PCM was found to melt and solidified after just 3 and ½ hrs(from 4:00pm to 7:36pm) due to high heat flux from the bulk of water all around it,representing 42% increase in heat retention time against a reference of 8 hours, and can support 116 Lts of water at the optimum temperature of 56.5^{o}C. For circumferential placement, the retention time significantly increased to 6.75 h representing 62.5%, and was found to support 225 Lts of water at optimal temperature of 61.7°C. For both central and circumferential the retention time increases further to 69% with capacity to support 245 Ltrs of water. Thus, it can be concluded that PCM located at the circumference has significant influence on heat retention time than conventional central PCMs and supports more volumes of water.

Received: 17-12-2025 / Accepted: 24-12-2026 / Published: 14-03-2026

https://doi.org/10.70118/ujet.2026.0301.22

4.3 Environmental Factors

The major factor considered is the solar radiation. Its peak intensity occur at 1 PM (spring > winter > summer > autumn). Daily irradiation modeled as I = -0.4188t^2 + 10.542t - 57.48 with an R^2=0.9954. The demand was higher in winter (low ambient temps) and lower in summer.

4.3.1 Energy Use and Economic Viability

Daily pump consumption was 2.02 kWh (15% lower than conventional systems). The average peak power achieved was 151.2 W (10 AM–2 PM) with a statistical reliability of MAE = 1.7°C (2.5% of target - 68°C), RMSE = 2.1°C, R^2 = 0.93.

The cost implication of the model covers the detailed modified bill of quantity shown in Table 2, based on an exchange rate of 1 USD being equivalent to N1,423.

Table 2: Cost Details of major units with Economic Viability

Parameter	Value (N)
Tank + PCM Cost	450,000
Insulation	150,000
Annual Savings	190,073
Payback Period (yrs)	2.3
Lifetime savings (10 yrs)	1,920,073

For Economic Viability, an upfront cost of ₦600,000 (tank/PCM: ₦450,000; insulation: ₦150,000) was used resulting to an annual savings of ₦192,073 and a payback = 2.3 years with lifetime (10y) net profit: ₦1,320,730 (220% ROI).

5.0 Conclusion

Circumferential PCM configuration optimizes heat retention in tropical climates. Dual PCM offers marginal gains over circumferential-only but significantly outperforms central-only systems. Economic analysis confirms viability with short payback (2.3 years). Recommendation: Adopt circumferential PCM in new/existing tanks for efficiency and energy savings.

References

[1] Oghogho, I., Sulaimon, O., Adedayo, B. A., Egbune, D. & Abanihi, K. V. (2014). "Solar Energy Potential And its Development for Sustainable Energy Generation In Nigeria: A Road Map to Achieving this Feat", *International Journal of Engineering and Management Sciences*, Vol.5 No. 2, pp.61-67.

[2] Chineke, T. C., Ozuomba, J. O., Anumaka, M. C., Ojiaka, J. C. & Akwuegbu, O. C. (2022) "Boosting the Harvesting of Nigeria's Abundant Renewable Energy Potentials and Legal Implications". *International Journal of Social Sciences*, 8(2022). Pp. 119-134.

[3] Haegel, M. N. & Kurtz, S. R. (2023). "Global Progress Toward Renewable Electricity: Tracking the Role of Solar, A Publication of IEE Electronic Devices", *IEEE Journal of Photovoltaic*, Doi:10.1109/JPHOTOV.

[4] Wheatley, M. C. (2024). "*Advancements in Renewable Energy Technologies: A Decade in Review*". *Premier Journal of Science*; 2024;1:100013. https://doi.org/10.70389/PJS.100013

[5] Liu, C., Zhao, Y. & Qu, Z. (2021). "Economic analysis of two kinds of water heaters in service industry". *EDP Sciences, E3S Web of Conferences* 257, 02059 (2021), https://doi.org/10.1051/e3sconf/202125702059

[6] Baddou, Y. (2017). "Solar thermal systems for domestic water heating applications in residential buildings.Efficiency and economic viability analysis of monitored plants'. *Master thesis in Renewable Energies and Energy Efficiency, UEMF-Morocco/UPC-Barcelona-Spain*.

[7] Khan, M. A., Sabahat, Z. Farooq, M. S., Saleem, M., Abbas, S., Ahmad, M., Mazhar, T., Shahzad, T. & Saeed M. M. ((2024). "Optimizing Smart Home Energy Management for Sustainability using Machine Learning Techniques". Journal of Research – Discover, Sustainability; 2024(, Vol. 5(430). https://doi.org/10.1007

[8]. Reddy, R. M., Nallusamy, N., & Reddy, K. H. (2012). "Experimental Studies on Phase Change Material-Based Thermal Energy Storage System for Solar Water Heating Applications". *Journal of Fundamentals of Renewable Energy and Applications* Vol. 2 (2012), Article ID R120314, pp. 1-6. https://doi:10.4303/jfrea/R120314

[9] Vijayan, A., & Hussain, J. (2016). "Experimental Analysis of Thermal Storage Systems using Phase Change Materials". *International Journal of Engineering Research & Technology (IJERT)*, Vol. 5 Issue 06, June-2016, pp. 789 – 797. www.ijert.org

[10] Podara, C. V., Kartsonakis, I. A. & Charitidis, C. A. (2021). "Towards Phase Change Materials for Thermal Energy Storage: Classification, Improvements and Applications in the Building Sector". *Applied Science*; 11, 1490. https://doi.org/10.3390/app11041490

[11] Sarcinella, A., Cunha, S., Aguiar, J. & M. Frigione, J. (2024). "ThermoChemical Characterization of Organic Phase Change Materials (PCMs) Obtained from Lost Wax Casting Industry". *Multidisciplinary Digital Publishing Institute Journals - Sustainability* 2024, 16, 7057. https://doi.org/10.3390/su16167057

Received: 17-12-2025 / Accepted: 24-12-2026 / Published: 14-03-2026

https://doi.org/10.70118/ujet.2026.0301.22

[12] El-Hanaf, A. (2025). "Thermal storage enhancement using phase change materials", *PhD Thesis submitted to Thermics [physics.class-ph], Université de Lorraine, 2025. Published by HAL Multi-disciplinary Science Open Access Archive*. https://hal.univ-lorraine.fr/tel-05226749v1

[13] Elkhatat, A. & Al-Muhtaseb, S. A. (2023). "Combined Renewable Energy–Thermal Energy Storage (RE–TES) Systems: A Review". Journal of *Energies* 2023, 16, 4471. https://doi.org/10.3390/en16114471

[14] Liu, M., Riahi, S., Sheoran, S., Brun, F., Jacob, R. & Belusko, M. (2021). *Techno-Economic Analysis of Thermal Energy Storage for Sensible and Latent Heat Systems as a Heat Source for CSP- Chapter 59, Global Emerging Innovation Summit (GEIS-2021), 2021, 528-554* ,Published by Bentham Science Publishers. https://creativecommons.org/licenses/by/4.0/legalcode

[15] Mofijur, M., Mahlia, T. M. I., Silitonga, A S., Silakhori, H. C. O. M., Hasan, M. H., Putra, N. & Rahman, S. M. A. (2019). "Phase Change Materials for Solar Energy Usages and Storage: An Overview". *Multidisciplinary Digital Publishing Institute - Energies* 2019, 12, 3167; doi:10.3390/en12163167 www.mdpi.com/journal/energies

[16] International Organization for Standardization (2018). "Solar Heating – Domestic Water Heating System-Part 2: Outdoor Testing Methods for System Performance Characterization and Yearly Performance Prediction of Solar only Systems". *International Standard Organization (ISO) 9459-2:1995(en).* https://www.iso.org/obp/ui/en#iso:std:17187:en

[17] Rashid, F. L., Dulaimi, A., Hatem, W. A., Al-Obaidi, M. A., Ameen, A., Eleiwi, M. A., Jawad, S. A., Bernardo L. F. A. & Hu J. W. (2024). "Recent Advances and Developments in Phase Change Materials in High-Temperature Building Envelopes: A Review of Solutions and Challenges". *Journal of Multidisciplinary Publishing Institute (MDPI) – Buildings;* 2024, 14, 1582. https://doi.org/10.3390/buildings14061582

[18] Kulish, V., Aslfattahi, N., Schmirler, M. & Sláma, P. (2023). "New library of phase-change materials with their selection by the Rényi entropy method"; *Journal of Nature - Scientific Reports;* vol. 13:10446. https://doi.org/10.1038/s41598-023-37701-0

[19] Nalla, B. T., Subbiah, G., Swarnkar, K. D., Das, K S. N., Kumar, S. M., Swarnka, S. K., Kaliappanand, N. & Priya, K. K. (2025). "Bio-based phase-change materials for thermal energy storage: Recent advances, challenges, and outlook"; *Results in Engineering*; 28 (2025) 107087, https://doi.org/10.1016/j.rineng.2025.107087

[20] Al-Yasiri, Q. & Szabó, M. (2021). "Performance Assessment of Phase Change Materials Integrated with Building Envelope for Heating Application in Cold Locations," *European Journal of Energy Research*, Vol 1, Issue 1, February 2021, http://dx.doi.org/10.24018/ejenergy.2021.1.1.5.

[21] Munir, M. U. & Hussain, A. (2022). "Thermal Stability Analysis of a PCM-Based Energy Storage System. Eng". *Proc. 2022, 23, 20*. https://doi.org/10.3390/engproc2022023020

[22] Adera, B., Ancha, V. R., Tadiwose T. & Getahun, E. (2025). "Nano enhanced phase change materials for thermal energy storage system applications: A comprehensive review of recent advancements and future challenges" *International Journal of Thermofluid*, 30 (2025), no. 101418, pp. 1 – 32.https://doi.org/10.1016/j.ijft.2025.101418

[23] Hopkins, P. E. (2021). "Bio-Based Phase Change Materials (PCMs) for Thermal Energy Storage," *U.S. Department of Energy's Office of Energy Efficiency and Renewable Energy (EERE), BTO's BENEFIT Program, Award number(s) DE-EE0009157*. Pp. 1-32.

[24] Das, A., Apu, M. H., Akter, A., Al-Rezaand M. M. & Mia, R. (2025). "An Overview of Phase Change Materials, their Production and Applications in Textiles. "Results in Engineering vol. 25 (2025) 103603. https://doi.org/10.1016/j.rineng.2024.103603.

[25] Mellouli, S., Alqahtani, T. & Algarni, S. (2022). "Parametric Analysis of a Solar Water Heater Integrated with PCMforLoadShifting". Multidisciplinary Publishing Institute (MDPI)-Energies 2022, 15, 8741. https://doi.org/10.3390/en15228741

[26] Modi, N., Wang, X. & Negnevitsky, M. (2023). "Solar Hot Water Systems Using Latent Heat Thermal Energy Storage: Perspectives and Challenges" Energies –Multidisciplinary Publishing Institute (MDPI) 2023, 16, 1969.https://doi.org/10.3390/en16041969

[27] Shah, D. A. (2024). "Phase Change Materials (PCMs) for passive Cooling: Performance in urban buildings" International Journal of Science and Research Archive, 2024, 13(01), pp. 3529-3548.https://doi.org/10.30574/ijsra.2024.13.1.2050

[28] Shukla, V. M., Singh, S. P. & Ranjan, A. (2024). "Design and Analysis of Pressure Vessel for Variable Thermal Load Considering Temperature, Material and Time Effects" Journal of Propulsion Technology, Vol. 45 No. 3 (2024), pp. 2381 – 2389.

[29] Kolhekar, R. R., Patil, H. D. & Gawande, T. K. (2016). "On Enhancing Efficiency of Solar Water Heater Using Phase Change Material"; International Journal of Innovative and Emerging Research in Engineering Vol. 3, Special Issue 1, ICSTSD 2016. Pp. 261 – 264.

[30] Benjamin, U. I., Shaibu, M., Lawal, M. N. & Ogo, O. E. (2024). The design optimization of a cold gas propellant tank pressurized system for nanosatellite. IMES, 1(1); pp. 1-6.

Received: 17-12-2025 / Accepted: 24-12-2026 / Published: 14-03-2026

https://doi.org/10.70118/ujet.2026.0301.22